crystals

MDPI

Article

Luminescence Properties of $Y_3F[Si_3O_{10}]$:Ln^{3+} (*Ln* = Eu, Tb, Er) with *Thalenite*-Type Host Lattice and Crystal Structure of $Tm_3F[Si_3O_{10}]$

Marion C. Schäfer [1,2], Michael Petter [1], Ingo Hartenbach [1,*], Ralf J. C. Locke [1], Shuang Zhang [3], Claudia Wickleder [3,*] and Thomas Schleid [1,*]

[1] Institute for Inorganic Chemistry, University of Stuttgart, D-70569 Stuttgart, Germany
[2] Patent Analyst at CPA Global (Clarivate), D-81541 München, Germany
[3] Institute for Inorganic Chemistry, University of Siegen, D-57068 Siegen, Germany
* Correspondence: ingo.hartenbach@iac.uni-stuttgart.de (I.H.); wickleder@chemie.uni-siegen.de (C.W.); thomas.schleid@iac.uni-stuttgart.de (T.S.)

Abstract: With $Tm_3F[Si_3O_{10}]$, a new representative of the $Ln_3F[Si_3O_{10}]$ series could be synthesized by the reaction of Tm_2O_3, TmF_3 and SiO_2 (molar ratio: 1:1:3), applying an excess of CsBr as a fluxing agent in gas-tightly sealed platinum crucibles for eight days at 750 °C, and designed to yield $Tm_3F_3[Si_3O_9]$ or $Cs_2TmF[Si_4O_{10}]$. Single crystals of $Tm_3F[Si_3O_{10}]$ (monoclinic, $P2_1/n$; a = 725.04(6), b = 1102.43(9), c = 1032.57(8) pm, β = 97.185(7)°; Z = 4) appear as pale celadon, transparent, air- and water-resistant rhombic plates. According to its *thalenite*-type structure, $Tm_3F[Si_3O_{10}]$ contains *catena*-trisilicate anions $[Si_3O_{10}]^{8-}$ and triangular $[FTm_3]^{8+}$ cations. The three crystallographically different Tm^{3+} cations are coordinated by seven *plus* one (Tm1) or only seven anions (Tm2 and Tm3) exhibiting a single F^- anion for each polyhedron, additional to the majority of O^{2-} anions. Furthermore, the luminescence properties of the isotypic colorless compound $Y_3F[Si_3O_{10}]$ doped with Eu^{3+} (red emission), Tb^{3+} (green emission) and Er^{3+} (yellow and infrared emission), respectively, are reported in presenting their different excitation and emission spectra.

Keywords: oxosilicates; fluorides; *thalenite*; crystal structure; luminescence

check for updates

Citation: Schäfer, M.C.; Petter, M.; Hartenbach, I.; Locke, R.J.C.; Zhang, S.; Wickleder, C.; Schleid, T. Luminescence Properties of $Y_3F[Si_3O_{10}]$:Ln^{3+} (*Ln* = Eu, Tb, Er) with *Thalenite*-Type Host Lattice and Crystal Structure of $Tm_3F[Si_3O_{10}]$. *Crystals* **2023**, *13*, 511. https://doi.org/10.3390/cryst13030511

Academic Editors: Alessandro Chiasera and László Kovács

Received: 10 February 2023
Revised: 9 March 2023
Accepted: 14 March 2023
Published: 16 March 2023

Copyright: © 2023 by the authors. Licensee MDPI, Basel, Switzerland. This article is an open access article distributed under the terms and conditions of the Creative Commons Attribution (CC BY) license (https://creativecommons.org/licenses/by/4.0/).

1. Introduction

In the quaternary systems RE_2O_3–REF_3–SiO_2 (*RE* = rare-earth element), only six different types of compounds are known so far, which can be distinguished by the linkage of the involved $[SiO_4]^{4-}$ tetrahedra via common vertices. The lanthanum fluoride oxosilicate $La_3F_3[Si_3O_9]$ [1,2] contains *cyclo*-trisilicate units $[Si_3O_9]^{6-}$ and therefore shows the highest degree of silicate connectivity. By breaking one of these bonds with an extra O^{2-} anion, the fluoride oxosilicates $RE_3F[Si_3O_{10}]$ (*RE* = Y [3], Dy–Er [4,5]) with a *thalenite*-type structure [6,7] are realized, which comprise *catena*-trisilicate units $[Si_3O_{10}]^{8-}$. Despite the assumption that only four representatives of this formula type [3–5] exist, it was recently possible to obtain the isotypic $Tm_3F[Si_3O_{10}]$ by a different synthetic route. Furthermore, the compound $RE_4F_2[Si_2O_7][SiO_4]$ (≡ "$RE_4F_2(Si_3O_{11}$"), *RE* = Y [8], Er [9]) is built-up by isolated *ortho*-oxosilicate ($[SiO_4]^{4-}$) and oxodisilicate units ($[Si_2O_7]^{6-}$) after another O^{2-} anion has torn the trisilicate chain fragment apart. Three isolated $[SiO_4]^{4-}$ tetrahedra occur in the mixed-valent fluoride *ortho*-oxosilicate $Eu_5F[SiO_4]_3$ (≡ "$Eu^{II}_2Eu^{III}_3F(Si_3O_{12})$") [10] with *apatite*-type structure, where all Si–O–Si bridges are lost. Moreover, discrete *ortho*-oxosilicate anions also dominate the structures of some oxide-fluoride derivatives, such as $La_7OF_7[SiO_4]_3$ [11] and $Sm_3OF_3[SiO_4]$ [12].

Silicate host lattices are very suitable for luminescence materials due to their generally excellent stability. Therefore, several different compounds doped with Eu^{3+}, Tb^{3+} and Er^{3+} were described in the past [13–20]. In this work, we use $Y_3F[Si_3O_{10}]$ as the host lattice

for the Ln^{3+} cations mentioned above and present their luminescence properties for the first time. Furthermore, the crystal structure of $Tm_3F[Si_3O_{10}]$, as a new compound of the *thalenite* series, is described in detail, since only lattice constants have been mentioned before [21].

2. Materials and Methods

Single crystals of $Tm_3F[Si_3O_{10}]$ have been synthesized by the reaction of thulium oxide (Tm_2O_3, ChemPur, Karlsruhe, Germany: 99.9%), thulium trifluoride (TmF_3, ChemPur, Karlsruhe, Germany: 99.9%) and silicon dioxide (SiO_2, Merck, Darmstadt, Germany: *silica gel*, *p. a.*) in a molar ratio of 1:1:3 with an excess of cesium bromide (CsBr, ChemPur, Karlsruhe, Germany: 99.9%) as the fluxing agent in gas-tightly sealed platinum ampoules (Horst zu Jeddeloh GmbH, Winsen/Luhe, Germany) for eight days at 750 °C. The original target products were $Tm_3F_3[Si_3O_9]$ or $Cs_2TmF[Si_4O_{10}]$, if Cs^+, as part of the flux, would become incorporated, as it happened in the case of $Cs_2YF[Si_4O_{10}]$ [22]. Following cooling by 10 °C/h down to room temperature and washing the crude product with water, the compound emerged as light green, transparent, air- and water-resistant rhombic plates. Crystallographic data of $Tm_3F[Si_3O_{10}]$ and details of its structural refinement, as well as atomic parameters and coefficients of the anisotropic thermal displacement factors are summarized in Tables 1 and 2. Selected interatomic distances and angles fill Tables 3 and 4 informs about the motifs of mutual adjunction [23,24].

Table 1. $Tm_3F[Si_3O_{10}]$: Crystallographic data and details of the structure refinement.

Crystal system and space group		monoclinic, $P2_1/n$ (no. 14)
Lattice parameters,	a/pm	725.04(6)
	b/pm	1102.43(9)
	c/pm	1032.57(8)
	β/°	97.185(7)
Formula units, Z		4
Calculated density, D_x/g·cm^{-3}		6.246
Molar volume, V_m/cm^3·mol^{-1}		123.28
Diffractometer and wavelength		κ-CCD (Bruker-Nonius), Mo-K_α: λ = 71.07 pm
$\pm h_{max}/\pm k_{max}/\pm l_{max}$		9/14/13
Θ_{max}/°		28.36
Electron sum, $F(000)$/e$^-$		1352
Absorption coefficient, μ/mm^{-1}		32.73
Absorption correction		*HABITUS* [27]
Reflections (unique)		23467 (2046)
R_{int}/R_σ		0.082/0.037
Reflections with $\lvert F_o \rvert \geq 4\sigma(F_o)$		2007
Structure determination and refinement		Programs *SHELXS-97* and *SHELXL-97* [28]
Scattering factors		International Tables, Vol. C [29]
R_1/R_1 with $\lvert F_o \rvert \geq 4\sigma(F_o)$		0.027/0.026
wR_2/Goodness of Fit (GooF)		0.060/1.181
Extinction coefficient, ε		0.0031(1)
Residual electron density, $\rho_{max/min}$/e$^-$ · 10^6 pm^{-3}		2.32/−2.65
CSD number		380467

Table 2. Atomic parameters and coefficients of the anisotropic thermal displacement factors (U_{ij}/pm^2) for $Tm_3F[Si_3O_{10}]$ (all atoms reside at the *Wyckoff* position 4*e*).

Atom	*x*/*a*	*y*/*b*	*z*/*c*	U_{11}	U_{22}	U_{33}	U_{23}	U_{13}	U_{12}	U_{eq}[a]/pm^2
Tm1	0.30151(4)	0.40156(3)	0.49629(3)	45(5)	79(2)	53(2)	0(1)	0(1)	−14(1)	60(1)
Tm2	0.40500(4)	0.27124(3)	0.81112(3)	50(2)	63(2)	42(2)	−2(1)	6(1)	4(1)	52(1)
Tm3	0.26348(4)	0.03200(3)	0.51734(3)	50(2)	72(2)	49(2)	−1(1)	1(1)	8(1)	57(1)
F	0.1957(6)	0.2150(4)	0.4397(4)	62(18)	62(20)	150(22)	17(15)	−21(15)	−7(15)	94(8)
Si1	0.0247(3)	0.0861(2)	0.7410(2)	32(8)	64(20)	32(8)	−5(6)	9(6)	3(6)	42(3)
Si2	0.2321(3)	0.2447(2)	0.1107(2)	23(8)	75(8)	47(8)	11(6)	11(6)	−5(6)	48(3)
Si3	0.4943(3)	0.0367(2)	0.2079(2)	24(8)	57(8)	47(8)	3(6)	6(6)	−4(6)	42(3)
O1	0.0134(7)	0.0252(5)	0.3630(5)	45(22)	73(23)	85(23)	−6(18)	−27(17)	−10(17)	71(9)
O2	0.0423(7)	0.0501(5)	0.8934(5)	44(21)	93(23)	46(21)	16(17)	−13(17)	44(17)	62(9)
O3	0.2099(7)	0.1431(5)	0.6967(5)	51(21)	84(23)	70(22)	7(18)	−7(17)	−29(18)	70(9)
O4	0.3448(7)	0.3225(5)	0.2319(5)	94(23)	103(24)	60(22)	9(19)	26(17)	−16(19)	84(9)
O5	0.2695(7)	0.3198(5)	0.9829(5)	123(23)	80(24)	49(22)	−2(19)	46(18)	11(19)	81(9)
O6	0.0155(7)	0.2277(4)	0.1200(5)	81(23)	83(24)	41(21)	0(17)	32(17)	−8(18)	66(9)
O7	0.3194(7)	0.1082(5)	0.1224(5)	45(21)	79(23)	97(23)	8(18)	−10(17)	5(17)	75(9)
O8	0.1860(7)	0.3946(5)	0.6927(5)	83(23)	72(23)	70(22)	12(18)	19(18)	17(18)	74(9)
O9	0.4666(7)	0.0208(5)	0.3621(5)	43(21)	127(24)	50(22)	11(18)	23(17)	2(18)	72(9)
O10	0.0267(7)	0.4103(5)	0.3721(5)	42(20)	81(24)	40(21)	17(18)	−16(16)	−35(17)	56(9)

[a] $U_{eq} = {}^1/_3\,[U_{22} + 1/\sin^2\beta(U_{11} + U_{33} + 2U_{13}\cdot\cos\beta)]$.

Table 3. Selected interatomic distances (*d*/pm) and bond angles (∢/°) for $Tm_3F[Si_3O_{10}]$.

	***d*/pm**		***d*/pm**		***d*/pm**
Tm1–F	224.7(4)	Tm2–F	235.1(4)	Tm3–F	220.4(4)
Tm1–O2	221.9(5)	Tm2–O5	219.9(5)	Tm3–O9	226.0(5)
Tm1–O2′	222.2(5)	Tm2–O6	222.1(5)	Tm3–O1	226.1(5)
Tm1–O10	223.3(4)	Tm2–O3	223.0(5)	Tm3–O3	229.4(5)
Tm1–O8	229.0(5)	Tm2–O10	224.5(5)	Tm3–O9′	231.2(5)
Tm1–O6	236.1(5)	Tm2–O8	232.0(5)	Tm3–O5	235.2(5)
Tm1–O7	268.2(5)	Tm2–O1	241.6(5)	Tm3–O1′	256.4(5)
Tm1–O4	292.0(5)				
Si1–O3	160.0(5)	Si2–O6	159.6(5)	Si3–O8	160.8(5)
Si1–O2	161.2(5)	Si2–O5	160.9(5)	Si3–O10	161.7(5)
Si1–O1	163.1(5)	Si2–O7	163.1(5)	Si3–O9	163.9(5)
Si1–O4	164.2(5)	Si2–O4	164.7(5)	Si3–O7	165.2(5)
	∢/°		∢/°		∢/°
O2–Si1–O4	99.9(3)	O4–Si2–O5	103.7(3)	O7–Si1–O10	97.0(3)
O1–Si1–O3	100.7(3)	O6–Si2–O7	105.2(3)	O7–Si1–O8	109.8(3)
O1–Si1–O4	110.9(3)	O4–Si2–O7	105.9(3)	O8–Si1–O9	111.0(3)
O2–Si1–O3	114.1(3)	O5–Si2–O6	112.2(3)	O8–Si1–O10	112.5(3)
O3–Si1–O4	115.6(3)	O4–Si2–O6	114.4(3)	O9–Si1–O10	112.9(3)
O1–Si1–O2	116.3(3)	O5–Si2–O7	115.6(3)	O7–Si1–O9	113.0(3)
Si1–O4–Si2	132.7(2)	Tm1–F–Tm2	109.9(2)		
Si2–O7–Si3	138.1(3)	Tm2–F–Tm3	114.1(2)		
		Tm1–F–Tm3	133.6(2)		

Table 4. Motifs of mutual adjunction [23,24] for the $Tm_3F[Si_3O_{10}]$ structure.

	F	O1	O2	O3	O4	O5	O6	O7	O8	O9	O10	*C.N.*
Tm1	1/1	0/0	2/2	0/0	0 + 1/0 + 1	0/0	1/1	1/1	1/1	0/0	1/1	**7 + 1**
Tm2	1/1	1/1	0/0	1/1	0/0	1/1	1/1	0/0	1/1	0/0	1/1	**7**
Tm3	1/1	2/2	0/0	1/1	0/0	1/1	0/0	0/0	0/0	2/2	0/0	**7**
Si1	0/0	1/1	1/1	1/1	1/1	0/0	0/0	0/0	0/0	0/0	0/0	**4**
Si2	0/0	0/0	0/0	0/0	1/1	1/1	1/1	1/1	0/0	0/0	0/0	**4**
Si3	0/0	0/0	0/0	0/0	0/0	0/0	0/0	1/1	1/1	1/1	1/1	**4**
C.N.	**3**	**4**	**3**	**3**	**2 + 1**	**3**	**3**	**3**	**3**	**3**	**3**	

The colorless samples for luminescence investigations $Y_3F[Si_3O_{10}]:Ln^{3+}$ (*Ln* = Eu, Tb, Er) could be synthesized via the classical route [3]. For this purpose, mixtures of yttrium oxide (Y_2O_3, ChemPur, Karlsruhe, Germany: 99.9%), yttrium trifluoride (YF_3, ChemPur, Karlsruhe, Germany: 99.9%) and silicon dioxide (SiO_2, Merck, Darmstadt, Germany: *silica gel*, *p. a.*) in the molar ratio 1:4:9 with a slight excess of cesium chloride (CsCl, ChemPur, Karlsruhe, Germany: 99.9%) as fluxing agent, and doped with 3% of the lanthanoid trifluorides LnF_3 (*Ln* = Eu, Tb, Er; each ChemPur, Karlsruhe, Germany: 99.9%) replacing YF_3, were heated in arc-sealed tantalum ampoules (Plansee, Reutte, Austria) for seven days at 700 °C. For example, to yield circa 500 mg of $(Y_{2.9}Er_{0.1})F[Si_3O_{10}]$, 271.36 mg of Y_2O_3 was mixed with 43.83 mg of YF_3, 2.25 mg of ErF_3 as dopant, and 168.06 mg of SiO_2 and a slight excess of cesium bromide (550 mg). The lack of color for $Y_3F[Si_3O_{10}]$ results from the fact that all included ions (Y^{3+} and Si^{4+} as well as F^- and O^{2-}) exhibit electronic closed-shell configurations ([Ne] for the anions and Si^{4+}, [Kr] for Y^{3+}). As no visible charge-transfer processes from the anions to the cations are active, there is no way to show any color within the 380–750-nm region. So consequently, all components or combinations, such as Y_2O_3, SiO_2, YF_3, SiF_4, YOF, $SiOF_2$ and $Y_2Si_2O_7$ appear colorless as well, no matter if covalent or ionic. For this reason, their huge band gaps feature the key property for energy preservation after irradiation followed by transfer processes and avoid thermal quenching. Since Y^{3+} as a non-lanthanoid cation exhibits the same ionic radius ($r_i(Y^{3+})$ = 96–102 pm for *C.N.* = 7–8) [25] as the mid-size Ln^{3+} cations, despite being so much lighter in weight, yttrium(III) compounds with "hard anions", such as F^- and O^{2-} according to the Pearson concept [26], provide perfect host materials for doping with luminescent Ln^{3+} guests with similar ionic radii, but open-shell representatives (e.g., Eu^{3+}: [Xe]$4f^6$, r_i = 101–107 pm; Tb^{3+}: [Xe]$4f^8$, r_i = 98–104 pm; Er^{3+}: [Xe]$4f^{11}$, r_i = 95–100 pm) [25] harvest the visible light upon UV irradiation from electronic *f*–*f* transitions.

Quick satisfying phase-purity checks with PXRD of each product were made with a STADI-P powder X-ray diffractometer (Stoe & Cie, Darmstadt, Germany; Cu-K_α radiation), but no Rietveld refinement appeared to be necessary (Figure 1). Semi-quantitative EDXS checks were made with an electron-beam X-ray microprobe (SX-100, Cameca, Gennevilliers, France) and Figure 2 shows a scanning electron micrograph of $Tm_3F[Si_3O_{10}]$. Photoluminescence emission and excitation spectra of each sample were recorded at room temperature on a Jobin Yvon fluorescence spectrometer (Fluorolog 3, Horiba, Kyoto, Japan) equipped with two 0.22 m double monochromators (SPEX, 1680, Horiba, Kyoto, Japan) and a 450 W xenon lamp. The emission spectra were corrected for photomultiplier sensitivity, the excitation spectra for lamp intensity and both for the transmission of the monochromators.

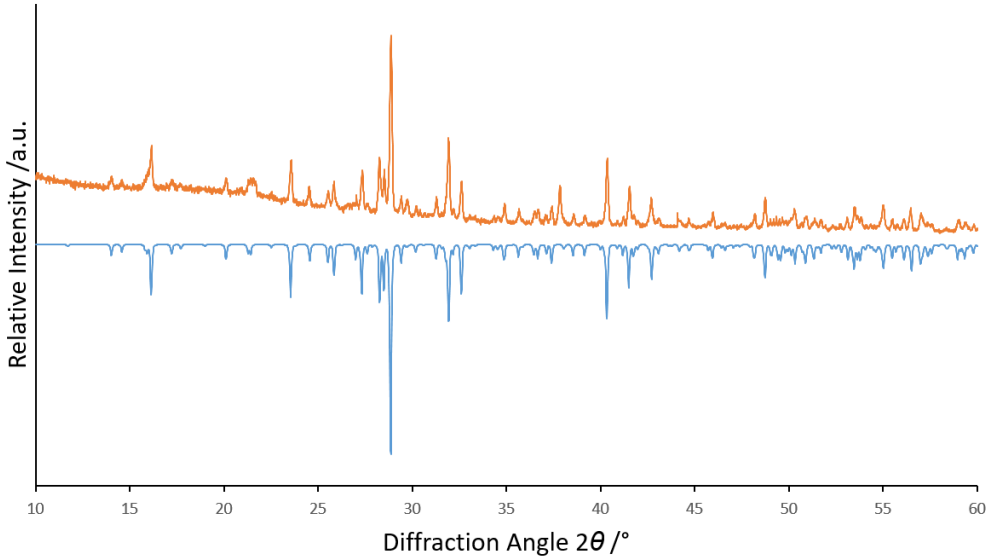

Figure 1. Powder X-ray diffractogram of $(Y_{2.9}Er_{0.1})F[Si_3O_{10}]$ (*top*: measured in orange, *bottom*: calculated in blue with data from [3]).

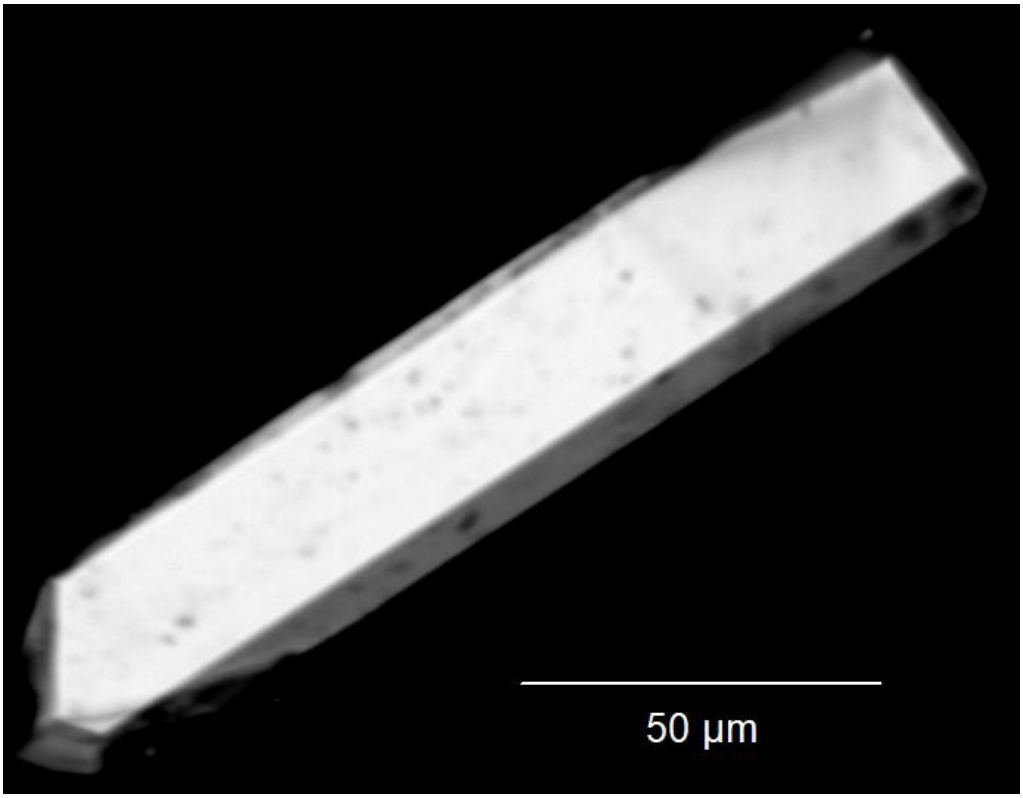

Figure 2. Scanning electron micrograph (SEM) of the measured, in this case bar-shaped, single crystal of $Tm_3F[Si_3O_{10}]$.

3. Results and Discussion

3.1. Structure Description

Instead of the expected hypothetical quinary thulium oxosilicate with the formula $Cs_2TmF[Si_4O_{10}]$, that was scheduled to form analogously to $Cs_2YF[Si_4O_{10}]$ [22], $Tm_3F[Si_3O_{10}]$ was surprisingly obtained in several experiments, which represents an extension of the domain of existence in the *thalenite*-type series ($RE_3F[Si_3O_{10}]$; *RE* = Dy, Ho, Er and Y [4,5]). $Tm_3F[Si_3O_{10}]$ crystallizes isotypically to monoclinic $Y_3F[Si_3O_{10}]$ [3] in space group $P2_1/n$

with a = 725.04(6), b = 1102.43(9), c = 1032.57(8) pm, β = 97.185(7)° and four formula units per unit cell. The three crystallographically independent $[SiO_4]^{4-}$ tetrahedra are linked via common vertices to an open, horseshoe-shaped chain fragment $[Si_3O_{10}]^{8-}$ (Figure 3), which has to be addressed as a *catena*-oxotrisilicate unit. The tetrahedra are aligned and eclipsed in respect to the O4 bridge (∢(Si1–O4–Si2) = 133°), but staggered considering the O7 connection (∢(Si2–O7–Si3) = 138°). In the unit cell, the opening of the $[Si_3O_{10}]^{8-}$ horseshoes is arranged alternatingly to the left and the right (Figure 4) along the [010] direction. The Si–O distances with values of 160–165 pm match very well with the distances of the two known types of thulium oxodisilicates (e.g., B-type $Tm_2Si_2O_7$: d(Si–O) = 160–165 pm [30] or C-type $Tm_2Si_2O_7$: d(Si–O) = 161–164 pm [31]). The triangular, almost planar, isolated $[FTm_3]^{8+}$ units (d(F–Tm) = 220–235 pm; Figure 5) are located between the $[Si_3O_{10}]^{8-}$ chain fragments (Figure 2). The deflection of the F^- anion from the $(Tm^{3+})_3$ triangle amounts to 20 pm and the Tm–F–Tm angles range from 110 to 134°. In the structure, three crystallographically distinguishable Tm^{3+} cations are found. $(Tm1)^{3+}$ is surrounded by one F^- and six *plus* one O^{2-} anions in the shape of a distorted square antiprism. The coordination polyhedra of $(Tm2)^{3+}$ can be described as a strongly distorted monocapped trigonal antiprism, consisting of one fluorine and six oxygen atoms and $(Tm3)^{3+}$ shows an environment of one F^- and six O^{2-} anions arranged as a distorted monocapped trigonal prism (Figure 5). The Tm–O distances with values of 220–268 *plus* 292 pm correspond excellently with those in thulium oxodisilicates, oxide *ortho*-oxosilicate or sulfide oxodisilicate, respectively (e.g., B-type $Tm_2Si_2O_7$: d(Tm–O) = 220–274 + 287 pm [30], $Tm_2O[SiO_4]$: d(Tm–O) = 218–250 + 322 pm [32], $Tm_4S_3[Si_2O_7]$: d(Tm–O) = 225–251 + 317 pm [33]). The distances between thulium and fluorine (d(Tm–F) = 220–235 pm) are also in good agreement with the separations in, for example, $BaTm_2F_8$ (d(Tm–F) = 222–231 pm) [34] or $TmF[AuF_4]_2$ (d(Tm–F) = 212–238 pm) [35]. For visualization of the crystal-structure features, Figures 3–5 were created using the DIAMOND [36] program.

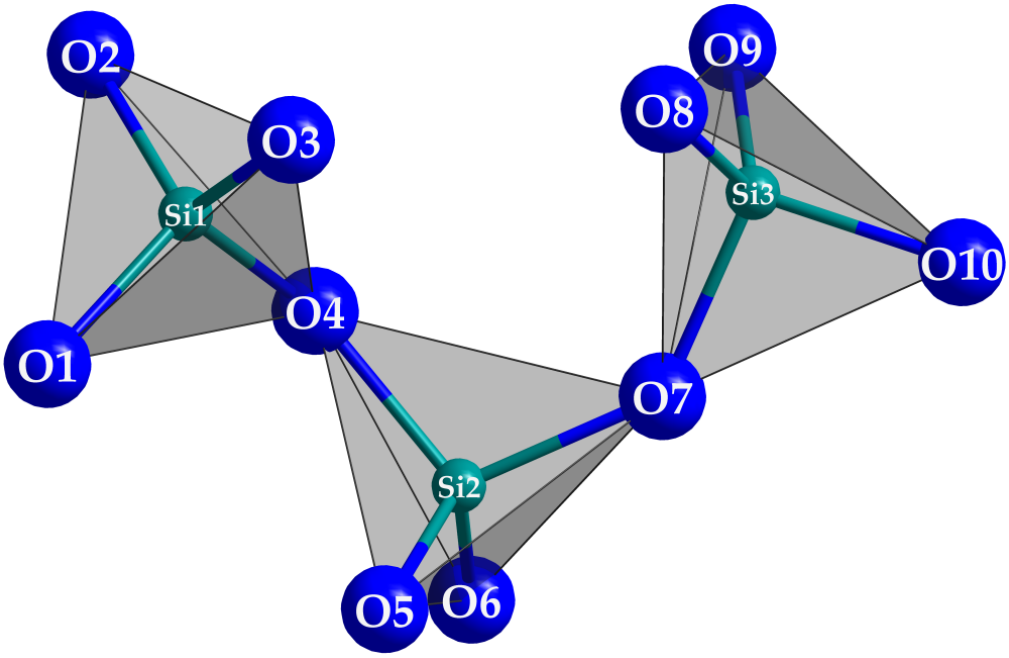

Figure 3. The horseshoe-shaped *catena*-oxotrisilicate anion $[Si_3O_{10}]^{8-}$ in $Tm_3F[Si_3O_{10}]$.

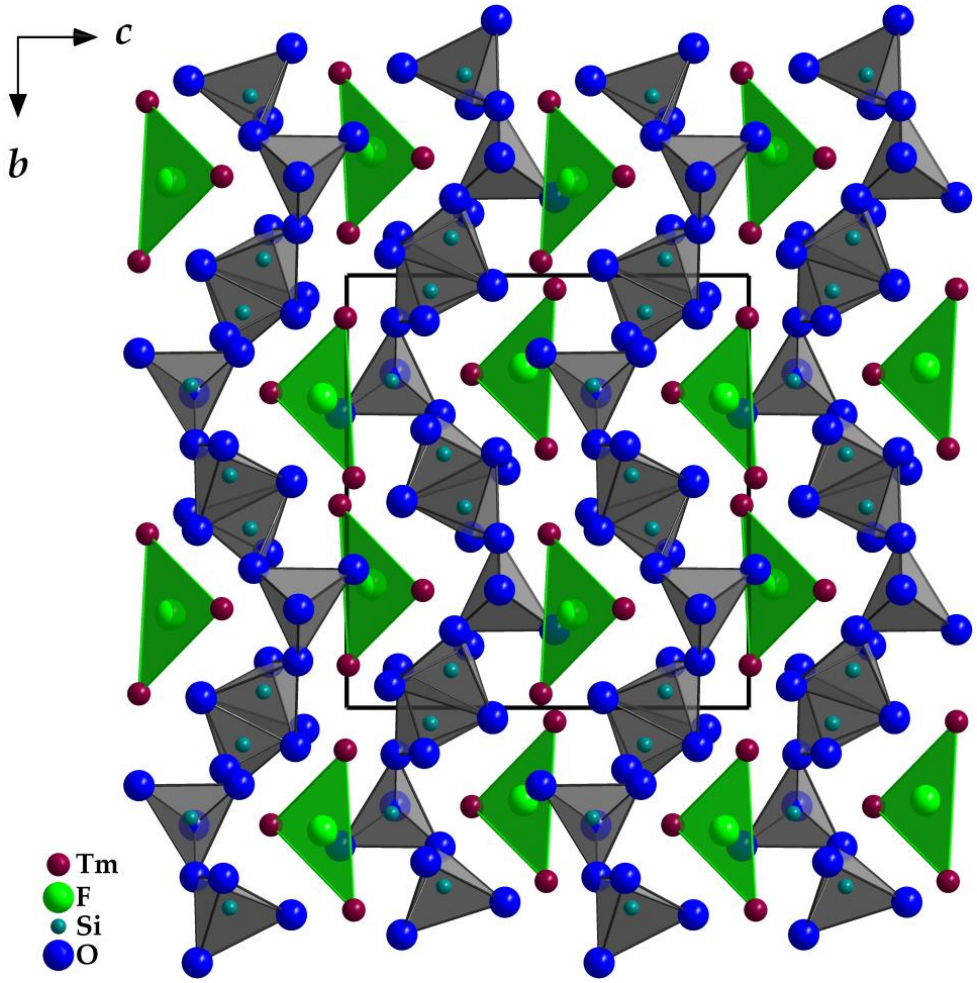

Figure 4. View at the monoclinic crystal structure of $Tm_3F[Si_3O_{10}]$ along [100] emphasizing the discrete $[FTm_3]^{8+}$ and $[Si_3O_{10}]^{8-}$ units.

3.2. Spectroscopy

In the $Y_3F[Si_3O_{10}]$:Ln^{3+} phosphors (*Ln* = Eu, Tb, Er), the doping Ln^{3+} cations are obviously able to replace all three different Y^{3+}-cation sites. The emission spectrum of $Y_3F[Si_3O_{10}]$:Eu^{3+} detected at 390 nm (Figure 6, *top*) presents strong peaks due to the $^5D_0 \rightarrow {}^7F_2$ transition, as well as the peaks for the $^5D_0 \rightarrow {}^7F_1$ transition. The $^7F_1$ level is split into nine components due to three different sites and the low symmetry for Eu^{3+} in the crystal structure. The existence of a weak $^5D_0 \rightarrow {}^7F_0$ peak indicates that only C_n, C_{nv} or C_s symmetries are possible. The bands for $^5D_1 \rightarrow {}^7F_J$ transitions were also observed. A weak broad band at 442 nm was detected, which suggests the occurrence of the charge-transfer transition O^{2-}-2*p* $\rightarrow$ Eu^{3+}-5*d*. The excitation spectrum detected at 585 nm (Figure 6, *bottom*) shows *f*–*f* transitions of the Eu^{3+} cation together with a broad band peaking at 316 nm, which can be assigned again to the $O^{2-} \rightarrow Eu^{3+}$ charge-transfer process.

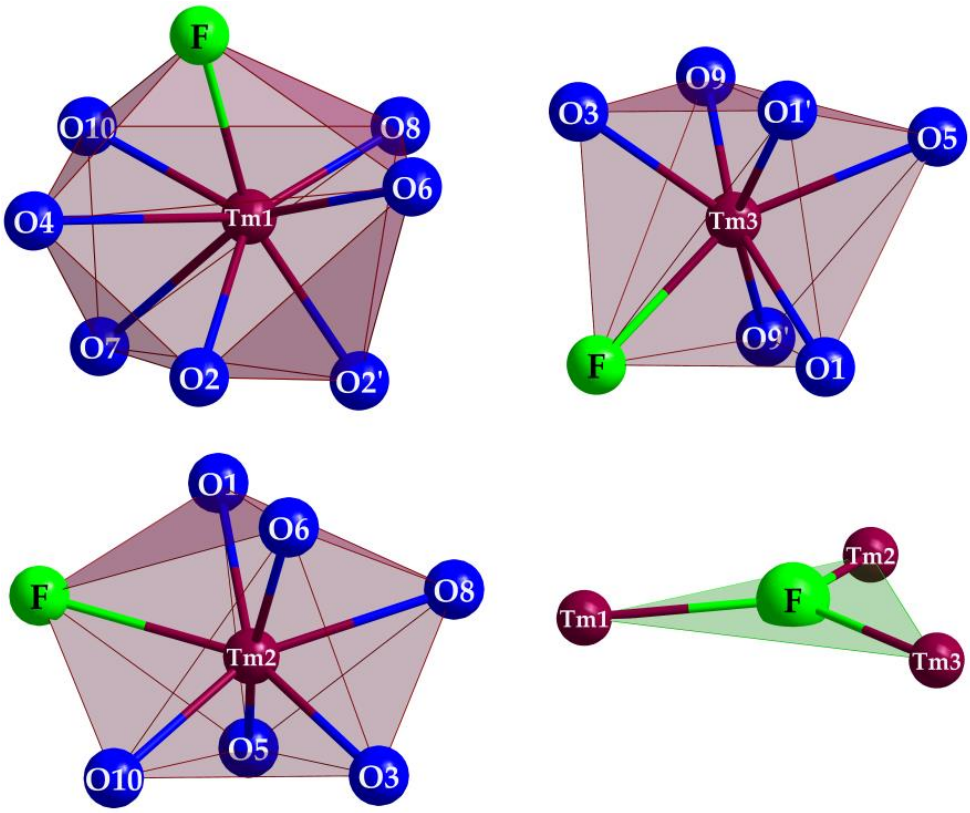

Figure 5. Coordination of the polyhedra of the three crystallographically independent Tm^{3+} cations and the triangular $[FTm_3]^{8+}$ unit in $Tm_3F[Si_3O_{10}]$.

In the emission spectrum of $Y_3F[Si_3O_{10}]$:Tb^{3+} at 370 nm (Figure 7, *top*), broad bands were detected for the $^5D_3 \rightarrow {}^7F_J$ and $^5D_4 \rightarrow {}^7F_J$ transitions. Due to the lot of degeneration possibilities of the *f*–*f* transitions, these bands usually appear to be broad. The excitation spectrum of $Y_3F[Si_3O_{10}]$:Tb^{3+} detected at 485 nm (Figure 7, *bottom*) shows the $^5D_3 \rightarrow {}^7F_6$ transition of Tb^{3+} together with an obvious strong broad band, which results from the allowed transition from the $4f^8$ to the $4f^75d^1$ configuration.

A large number of bands between 536 and 550 nm were detected for $^4S_{3/2} \rightarrow {}^4I_{15/2}$ in the emission spectrum of $Y_3F[Si_3O_{10}]$:Er^{3+} at 375 nm (Figure 8, *top*). The excitation spectrum (Figure 8, *bottom*) recorded at 536 nm shows strong peaks due to *f*–*f* transitions. This indicates that the luminescence of Er^{3+} is almost exclusively owed to *f*–*f* transitions of the Er^{3+} cations.

Figure 9 shows that $Y_3F[Si_3O_{10}]$:Er^{3+} also offers infrared emission bands, the strongest at 850 nm ($\equiv$ 11765 cm^{-1}), 1000 nm ($\equiv$ 10000 cm^{-1}), 1200 nm ($\equiv$ 8333 cm^{-1}) and 1500 nm ($\equiv$ 6667 cm^{-1}), which can be attributed to $^4S_{3/2} \rightarrow {}^4I_{13/2}$, $^4I_{11/2} \rightarrow {}^4I_{15/2}$, $^4F_{9/2} \rightarrow {}^4I_{13/2}$ and $^4I_{13/2} \rightarrow {}^4I_{15/2}$ transitions, respectively. However, this special kind of Er^{3+} IR-luminescence seems more suitable for living tissue probing [37] than for lighting applications.

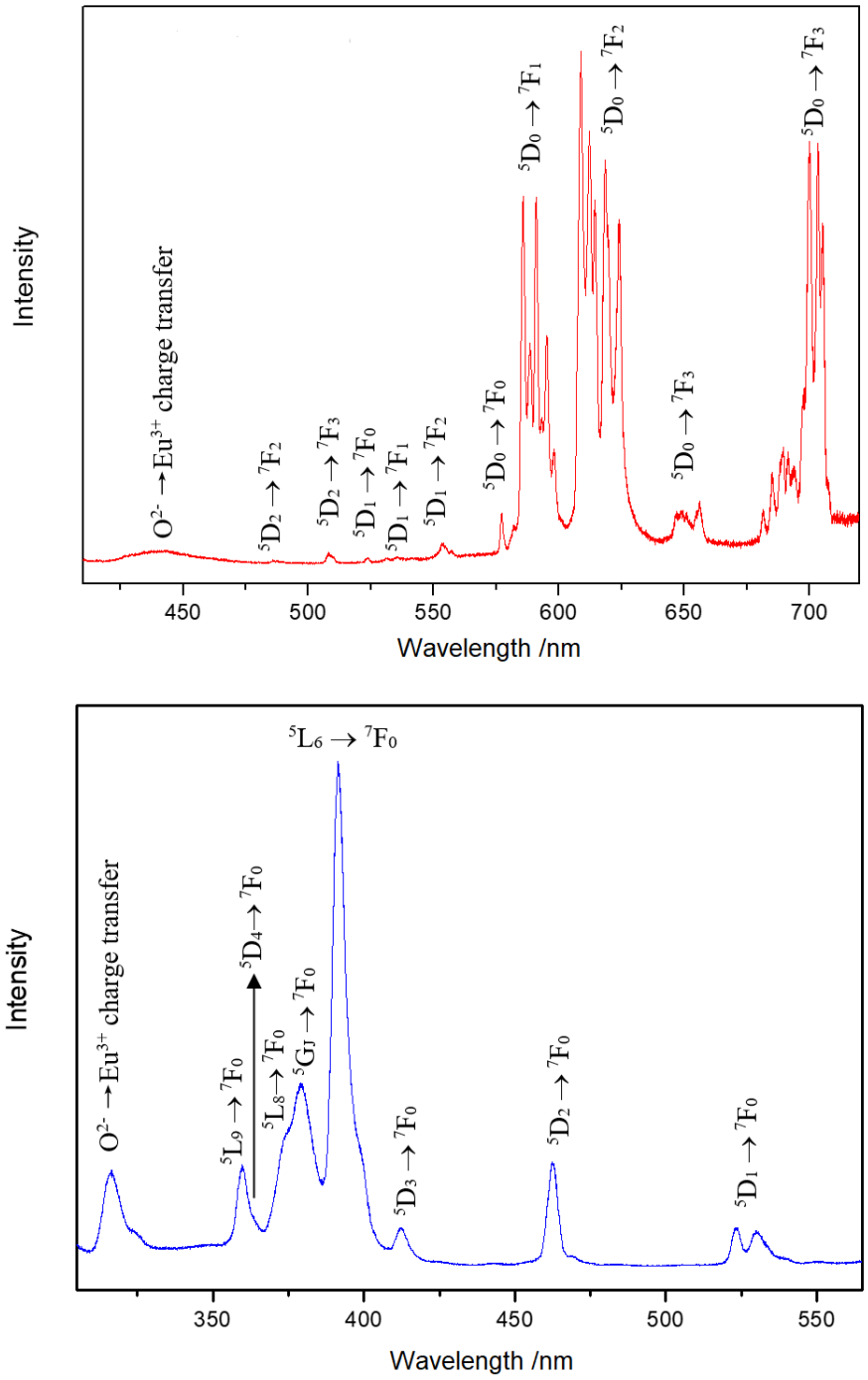

Figure 6. Emission spectrum of $Y_3F[Si_3O_{10}]:Eu^{3+}$ excited at 390 nm at room temperature (*top*). Excitation spectrum of $Y_3F[Si_3O_{10}]:Eu^{3+}$ detected at the emission energy of 585 nm at room temperature (*bottom*).

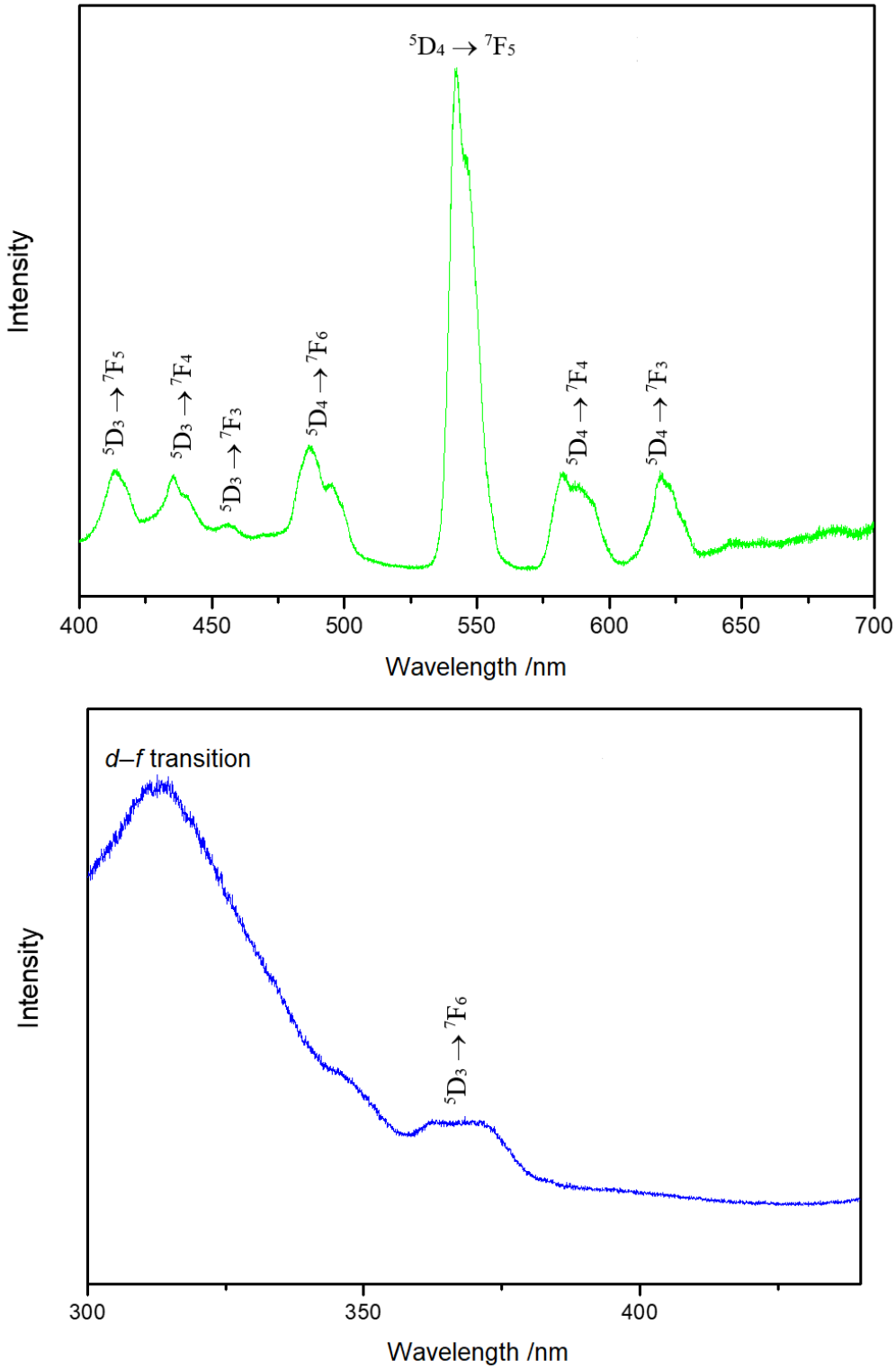

Figure 7. Emission spectrum of $Y_3F[Si_3O_{10}]:Tb^{3+}$ excited at 370 nm at room temperature (*top*). Excitation spectrum of $Y_3F[Si_3O_{10}]:Tb^{3+}$ detected at the emission energy of 485 nm at room temperature (*bottom*).

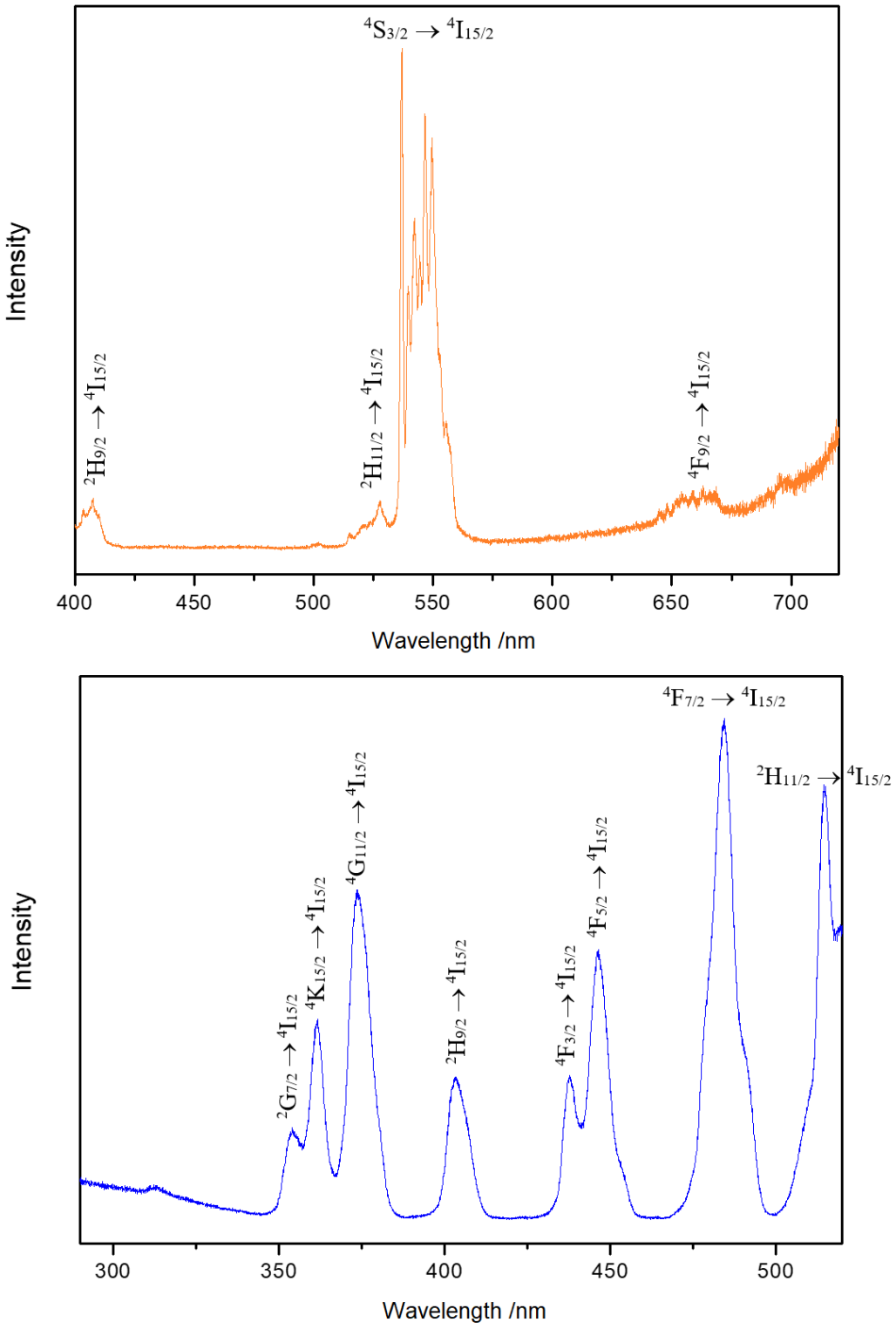

Figure 8. Emission spectrum of $Y_3F[Si_3O_{10}]:Er^{3+}$ excited at 375 nm at room temperature (*top*). Excitation spectrum of $Y_3F[Si_3O_{10}]:Er^{3+}$ detected at the emission energy of 536 nm at room temperature (*bottom*).

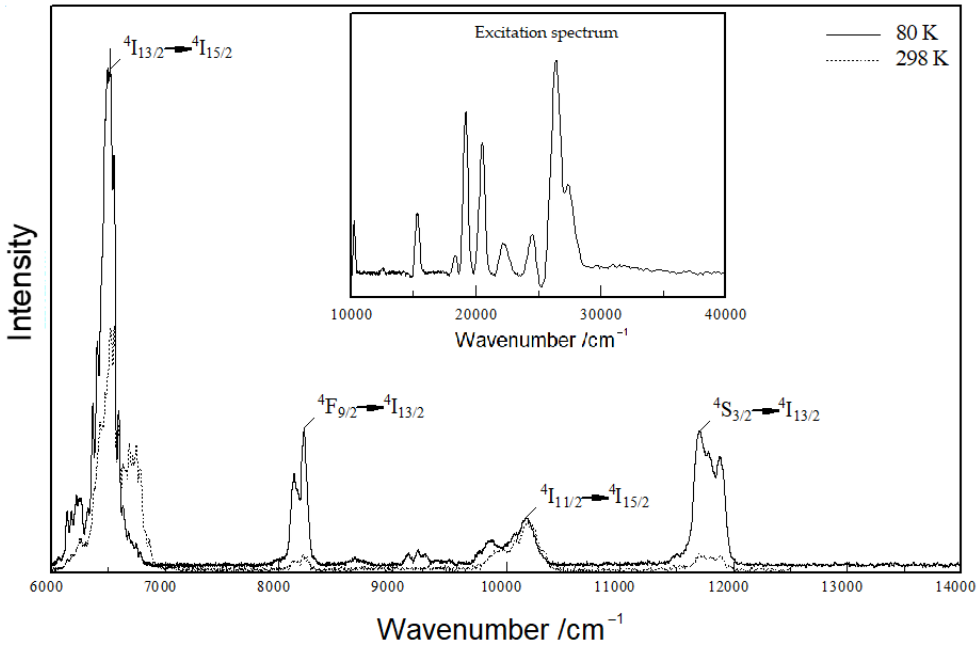

Figure 9. Emission spectrum of $Y_3F[Si_3O_{10}]:Er^{3+}$ excited at 375 nm at room temperature (*dotted curve*) and 80 K (*solid curve*); excitation spectrum inserted of $Y_3F[Si_3O_{10}]:Er^{3+}$ detected at the emission energy of 536 nm at room temperature.

4. Conclusions

The crystal structure of $Tm_3F[Si_3O_{10}]$ is presented for the first time with the so far heaviest Ln^{3+} cation of the $Ln_3F[Si_3O_{10}]$ series (*Ln* = Dy–Tm), exhibiting the monoclinic *thalenite*-type arrangement of $Y_3F[Si_3O_{10}]$. The latter itself was used for doping experiments with selected Ln^{3+} cations replacing 3% of its Y^{3+} content. With Eu^{3+} as dopant, the typical red luminescence resulting from $^5D_0 \rightarrow {}^7F_2$ and $^5D_0 \rightarrow {}^7F_1$ transitions could be detected and interpreted, while the Tb^{3+}- and Er^{3+}-doped $YF_3[Si_3O_{10}]$ samples shine green and yellow light, respectively, accompanied by rather strong emissions in the infrared region for the Er^{3+} case.

Author Contributions: Conceptualization, M.C.S. and T.S.; methodology, M.C.S., M.P. and S.Z.; software, M.C.S. and S.Z.; validation, M.C.S., T.S. and C.W.; formal analysis, M.C.S., T.S. and C.W.; investigation, M.C.S., T.S. and C.W.; resources, T.S. and C.W.; data curation, M.C.S., T.S., S.Z. and C.W.; writing—original draft preparation, M.C.S., I.H., R.J.C.L., C.W. and T.S.; writing—review and editing, M.C.S., I.H., R.J.C.L., C.W. and T.S.; visualization, M.C.S., S.Z., R.J.C.L. and I.H.; supervision, T.S.; project administration, T.S.; funding acquisition, C.W. and T.S. All authors have read and agreed to the published version of the manuscript.

Funding: We gratefully acknowledge the State of Baden-Württemberg (Stuttgart) for financial support. Moreover, we are thankful for the funding from the Deutsche Forschungsgemeinschaft (Bonn) within the SFB 1166 priority program "lanthanoid-specific functionalities in molecule and material".

Institutional Review Board Statement: Not applicable.

Informed Consent Statement: Not applicable.

Data Availability Statement: All the data supporting the conclusions are included within the manuscript and available upon request from the corresponding authors.

Acknowledgments: We thank Falk Lissner for the single-crystal X-ray diffraction measurement.

Conflicts of Interest: The authors declare no conflict of interest.

References

1. Müller-Bunz, H.; Schleid, T. $La_3F_3[Si_3O_9]$: Ein Fluorid-*cyclo*-Trisilicat des Lanthans. *Z. Kristallogr.* **1997**, *S12*, 141.
2. Müller-Bunz, H.; Schleid, T. $La_3F_3[Si_3O_9]$: Das erste Fluoridsilicat aus dem tenären System $LaF_3/La_2O_3/SiO_2$. *Z. Anorg. Allg. Chem.* **1999**, *625*, 1377–1383. [CrossRef]
3. Schleid, T.; Müller-Bunz, H. Einkristalle von $Y_3F[Si_3O_{10}]$ im *Thalenit*-Typ. *Z. Anorg. Allg. Chem.* **1998**, *624*, 1082–1084. [CrossRef]
4. Schleid, T.; Müller-Bunz, H. $Er_3F[Si_3O_{10}]$: Ein Fluorid-*catena*-Trisilicat des Erbiums. *Z. Kristallogr.* **1997**, *S12*, 134.
5. Müller-Bunz, H.; Schleid, T. Darstellung und Aufbau der Lanthanoidfluorid-*catena*-Trisilicate $M_3F[Si_3O_{10}]$ (M = Dy, Ho, Er) im Fluorthalenit-Typ ($Y_3F[Si_3O_{10}]$). *Z. Anorg. Allg. Chem.* **2000**, *626*, 845–852. [CrossRef]
6. Kornev, A.N.; Batalieva, N.G.; Maksimov, B.A.; Ilyukhin, V.V.; Belov, N.V. Crystalline structure of thalenite, $Y_3[Si_3O_{10}](OH)$. *Dokl. Akad. Nauk SSSR* **1972**, *202*, 1324–1327.
7. Yakubovich, O.V.; Voloshin, A.V.; Pakhomovskii, Y.A.; Simonov, M.A. Refined crystal structure of thalenite. *Kristallografiya* **1988**, *33*, 605–608.
8. Schäfer, M.C.; Hartenbach, I.; Schleid, T. Tetrayttrium difluoride disilicate orthosilicate, $Y_4F_2[Si_2O_7][SiO_4]$. *Acta Crystallogr.* **2013**, *E69*, i71. [CrossRef]
9. Müller-Bunz, H.; Schleid, T. $Er_4F_2[Si_2O_7][SiO_4]$: Das erste Selten-Erd-Fluoridsilicat mit zwei verschiedenen Silicat-Anionen. *Z. Anorg. Allg. Chem.* **2001**, *627*, 218–223. [CrossRef]
10. Wickleder, C.; Hartenbach, I.; Lauxmann, P.; Schleid, T. $Eu_5F[SiO_4]_3$ und $Yb_5S[SiO_4]_3$. *Z. Anorg. Allg. Chem.* **2002**, *628*, 1602–1606. [CrossRef]
11. Müller-Bunz, H.; Schleid, T. $La_7OF_7[SiO_4]_3$: Das erste Selten-Erd-Oxidfluorid-*ortho*-Silicat. *Z. Kristallogr.* **2002**, *S19*, 115.
12. Zimmerhofer, F.; Netzer, F.; Tribus, M.; Huppertz, H. Crystal strucuture determination and characterization of $Sm_3SiO_5F_3$. *Z. Naturforsch.* **2022**, *77b*, 657–665. [CrossRef]
13. Cannas, C.; Mainas, M.; Musinu, A.; Piccaluga, G.; Speghini, A.; Bertinelli, M. Nanocrystalline luminescent Eu^{3+}-doped Y_2SiO_5 prepared by sol-gel technique. *Opt. Mater.* **2005**, *27*, 1506–1510. [CrossRef]
14. Zhang, W.; Xie, P.; Duan, C.; Yan, K.; Yin, M.; Lou, L.; Xia, S.; Krupa, J.-C. Preparation and size effect on concentration quenching of nanocrystalline Y_2SiO_5:Eu. *Chem. Phys. Lett.* **1998**, *292*, 133–136. [CrossRef]
15. Ananias, D.; Ferdov, S.; Paz, F.A.A.; Sa Ferreira, R.A.; Ferreira, A.; Geraldes, C.F.G.C.; Carlos, L.D.; Lin, Z.; Rocha, J. Photoluminescent Layered Lanthanide Silicate Nanoparticles. *Chem. Mater.* **2008**, *20*, 205–212. [CrossRef]
16. Reichardt, J.; Stiebler, M.; Hirrle, R.; Kemmler-Sack, S. Cathodo- and Photoluminescence in Oxyorthosilicates of X_1 and X_2 Type: System $Y_{2-x}Gd_xSiO_5$: Tb^{3+}. *Phys. Stat. Sol.* **1990**, *A119*, 631–642. [CrossRef]
17. Lammers, M.J.J.; Blasse, G. Luminescence of Tb^{3+}-and Ce^{3+}-Activated Rare Earth Silicates. *J. Electrochem. Soc.* **1987**, *134*, 2068–2072. [CrossRef]
18. Ding, Y.; Zhao, G.; Xu, X. Crystal growth and spectroscopic properties of erbium doped Lu_2SiO_5. *J. Cryst. Growth* **2010**, *312*, 2103–2106. [CrossRef]
19. Hayhurst, T.; Shalimoff, G.; Edelstein, N.M.; Boatner, L.A.; Abraham, M.M. Optical spectra and Zeeman effect for Er^{3+} in $LuPO_4$ and $HfSiO_4$. *J. Chem. Phys.* **1981**, *74*, 5449–5452. [CrossRef]
20. Oskam, K.D.; Kaspers, K.A.; Meijerink, A.; Müller-Bunz, H.; Schleid, T. Luminescence of $La_3F_3[Si_3O_9]$:Ce^{3+}. *J. Lumin.* **2002**, *99*, 101–105. [CrossRef]
21. Schleid, T.; Müller-Bunz, H.; Janka, O. Geo-Inspired Phosphors Based on Rare-Earth Metal(III) Fluorides with Complex Oxoanions: I. Fluoride Oxocarbonates and Oxosilicates. In *Minerals as Advanced Materials II*; Krivovichev, S.V., Ed.; Springer: Berlin, Heidelberg, Germany, 2011; pp. 353–366.
22. Schäfer, M.C.; Schleid, T. Synthese und Kristallstruktur des Fluorid-*ino*-Oxosilicats $Cs_2YFSi_4O_{10}$. *Z. Anorg. Allg. Chem.* **2007**, *633*, 1018–1023. [CrossRef]
23. Hoppe, R. The Coordination Number — An "Inorganic Chameleon". *Angew. Chem. Int. Ed.* **1970**, *9*, 25–34. [CrossRef]
24. Hoppe, R. On the Symbolic Language of the Chemist. *Angew. Chem. Int. Ed.* **1980**, *19*, 110–125. [CrossRef]
25. Shannon, R.D. Revised Effective Ionic Radii and Systematic Studies of Interatomic Distances in Halides and Chalcogenides. *Acta Crystallogr.* **1975**, *A32*, 751–767. [CrossRef]
26. Pearson, R.G. Hard and Soft Acids and Bases. *J. Am. Chem. Soc.* **1963**, *85*, 3533–3539. [CrossRef]
27. Herrendorf, W.; Bärnighausen, H. *HABITUS: Program for the Optimization of the Crystal Shape for Numerical Absorption Correction in X-SHAPE*; Version 1.06; Fa. Stoe: Darmstadt, Germany, 1999.
28. Sheldrick, G.M. *SHELXS-97 and SHELXL-97: Programs for Solution and Refinement of Crystal Structures from X-ray Diffraction Data*; University of Göttingen: Göttingen, Germany, 1997.
29. Wilson, A.J.C. (Ed.) *International Tables for Crystallography*, 2nd edit.; Kluwer Academic Publishers: Boston, MA, USA; Dordrecht, The Netherlands; London, UK, 1992; Volume C.
30. Hartenbach, I.; Lissner, F.; Schleid, T. Crystal Structure of B-Type $Tm_2Si_2O_7$ ($\equiv Tm_4[Si_3O_{10}][SiO_4]$). *Z. Naturforsch.* **2003**, *58b*, 925–927. [CrossRef]
31. Felsche, J. Polymorphism and crystal data of the rare-earth disilicates of type $RE_2Si_2O_7$. *J. Less-Common Met.* **1970**, *21*, 1–14. [CrossRef]
32. Müller-Bunz, H.; Schleid, T. Über die Oxidsilicate $M_2O[SiO_4]$ der schweren Lanthanoide (M = Dy–Lu) im A-Typ. *Z. Anorg. Allg. Chem.* **1999**, *625*, 613–618. [CrossRef]

33. Sieke, C.; Hartenbach, I.; Schleid, T. Sulfidisch derivatisierte Oxodisilicate der schweren Lanthanide vom Formeltyp $M_4S_3[Si_2O_7]$ (M = Gd–Tm). *Z. Naturforsch.* **2002**, *57b*, 1427–1432. [CrossRef]
34. Izotova, O.E.; Aleksandrov, V.B. Crystalline Structure of $BaTm_2F_8$. *Dokl. Akad. Nauk SSSR* **1970**, *192*, 1037–1039.
35. Engelmann, U.; Müller, B.G. Tetrafluoroaurate(III) der Lanthaniden $MF[AuF_4]_2$ (M = Tm, Yb, Lu). *Z. Anorg. Allg. Chem.* **1993**, *619*, 1661–1668. [CrossRef]
36. Crystal Impact GbR. *DIAMOND: Visual Crystal Structure Information System*; Crystal Impact GbR: Bonn, Germany, 1999.
37. Cao, C.; Xie, Y.; Li, S.-W.; Hong, C. Er^{3+}-Ions-Doped Multiscale Nanoprobes for Fluorescence Imaging in Cellular and Living Mice. *Nanomaterials* **2021**, *11*, 2676. [CrossRef] [PubMed]

Disclaimer/Publisher's Note: The statements, opinions and data contained in all publications are solely those of the individual author(s) and contributor(s) and not of MDPI and/or the editor(s). MDPI and/or the editor(s) disclaim responsibility for any injury to people or property resulting from any ideas, methods, instructions or products referred to in the content.